ELSEVIER

Thermochimica Acta 269/270 (1995) 779–795

thermochimica acta

Characterization of ancient, byzantine and later historic mortars by thermal and X-ray diffraction techniques ☆

A. Moropoulou [a,*], A. Bakolas [b], K. Bisbikou [a]

[a] *Department of Material Science and Engineering, National Technical University of Athens, 9 Iroon Polytechniou, 15773 Athens, Greece*

[b] *Dipartimento di Scienze Ambientali, Universita di Venezia, 2137 Calle Larga S. Marta, 30123 Venezia, Italy*

Received 16 September 1994; accepted 9 June 1995

Abstract

The characterization of mortar properties can be accomplished by the use of thermal analysis. DTA can be used to identify various component materials and observe the reactions associated with controlled heating of the mortar. This method reveals thermal transformations, which include dehydration, dehydroxylation, oxidation and decomposition. In addition, crystalline transitions can be observed, which are exothermic or endothermic in nature. With TGA, thermogravimetric analysis, the mass of the sample is monitored (weight loss) as a function of temperature. Weight losses at reaction temperatures near 750°C, indicate loss of CO_2 not from pure $CaCO_3$, but from recarbonated lime.

The dehydroxylated clays acted as a "pozzolan" which imparts early strength to the mortar. However, a more complex phenomenon occurs in crushed brick mortar, since compounds of hydraulic type occur at the brick matrix interface also. The DTA and TG–DTG analyses identify the dehydration of calcium alumino-silicate phases, giving clear evidence of a cementitious mortar rather than one of pure lime.

In the present work a spectrum of thermal and XRD analysis results from ancient, Byzantine, post-Byzantine and later historic mortars from Greece is presented and the relevant information concerning the characterization of traditional mortars is validated

Generally, the CO_2 bound to carbonates and the water bound to hydraulic components (in weight loss%) discern two groups of mortars, the typical lime and the hydraulic, respectively. The specific classification of mortars into groups with characteristic transformations indicated by weight loss against temperature, enables discernment of: typical lime, cementitious, with crushed

* Corresponding author.

☆ Presented at the 6th European Symposium on Thermal Analysis and Calorimetry, Grado, Italy, 11–16 September 1994.

0040-6031/95/$09.50 © 1995 – Elsevier Science B.V. All rights reserved
SSDI 0040-6031(95)02571-5

brick, with portlandite, with gypsum, with modern cement or of hot lime technology, mortars. Mineralogical, microstructural, mechanical and technological data could provide further evaluation criteria.

Keywords: Cementitious mortars; Crushed brick mortars; Gypsum mortars; Historic mortars; Hydraulicity; Modern cement mortars; Portlandite mortars; TG–DTG evaluation; Thermal transformation; Typical lime mortars

1. Introduction

References cited in literature indicate that DTA, along with TG, X-ray diffraction techniques, electron microscopy and high-temperature microscopy; is indispensable to all aspects of the production and application of cementitious materials [1]. More specifically, this kind of analysis could be useful for the identification of mortars and for determination of the degree of hydration and carbonation of limes in mortars. Furthermore, the recarbonation properties of limestone can be systematically and dependably studied using controlled atmosphere techniques. Hence, in the case of historic mortars, thermal analysis could serve as a tool in their characterization, in the process of evaluation of their state and in reverse engineering research for the production of mortars used for restoration. In particular, historic mortars are complex systems, in which the binding to inert material is not easily identifiable, and where a limited amount of sample does not always permit physical separation into fragments [2].

DTA could be used to identify various component materials of a non-fractioned mortar and to observe the reactions associated with controlled heating of the mortar. This method reveals thermal transformation, exothermic or endothermic in nature, including dehydration, dehydroxylation, oxidation and decomposition. In combination with TGA, the weight loss of the sample monitored as a function of temperature, the classification of mortars should be further investigated.

With regard to clay minerals, the endothermic peak around 100°C is due to hygroscopic water (i.e. physically adsorbed water), whereas those appearing at about 200–250°C are attributed to "bound water" or to "hydrated interlayer cations". Gypsum, if present, also shows endothermic effects within the range of 120–200°C; because of the characteristic nature of the gypsum peaks, Wiedmann [3] considers that dehydration studies can be employed for quantitative and qualitative determination of impurities in raw materials used in the gypsum industry. Related to this is the work of Holdridge [4], which used DTA to characterize gypsum plasters. Water bound to aluminosilicates is detected by the endothermic peaks of dehydration between 200 and 650°C.

$Ca(OH)_2$ dehydration is detected between 400 and 520°C. Calcite and aragonite can be conveniently differentiated by virtue of the non-reversible phase change that occurs at about 470°C for aragonite [1].

The most common clay minerals (kaolinite, illite, smectite) are recognizable by their relatively strong endothermic effects within the range 500–650°C, followed by dehyd-

roxylation. DTA and TG analyses identify the dehydration of calcium aluminosilicate phases, giving clear evidence of a cementitious mortar rather than one of a pure lime. The $\alpha \rightarrow \beta$ phase transition of quartz is detected at about 580°C. Also organic matter used as an additive to promote carbonation and to improve workability, setting time and durability of the mortars) can produce exothermic effects within the range 300–500°C [2].

Carbonates show distinctive endothermic peaks: at around 840°C (calcite) and doublets at around 780°C and at 860°C (dolomite), whose position may vary depending on grain size, atmosphere and other concomitant factors. They are due to the escape of CO_2 during the breakdown of their structure. DTA is also capable of differentiating high-calcium limestones, dolomites and intermediate materials such as dolomitized limestones [1].

In lime used in building it is important that the magnesia should be hydrated, since in its unhydrated form it is the component most likely to lead to unsoundness. In addition, magnesia hydrated in lime contributes substantially to desirable plasticity. However, its dehydration could be identified at 250-280°C (hydromagnesite), 350–420°C (magnesia hydrate), while magnesium carbonates decompose in the range 450–520°C and calcium carbonate, associated with it, in the range 700–900°C [2].

Weight losses at reaction temperatures near 750°C, indicate the loss of CO_2 not from pure $CaCO_3$, but from recarbonated lime which includes some cementitious material, in the case that the original limestone contained suitable clay minerals, the hydration of which might have contributed to the CAH (calcium aluminate hydrate) or CSH (calcium silicate hydrate) phases. Studies of the medieval mortars from the Gothic cathedrals of France gives evidence of early decomposition of $CaCO_3$ to CO_2 between 663–713°C, revealing that illite, present in the Paris basin, became dehydroxylated during the lime burning process [5]. These dehydroxylated clays acted as a "pozzolan" imparting early strength to the mortar. However, a more complex phenomenon occurs in the crushed brick mortar, since compounds of hydraulic type take place at the brick matrix interface as well [6].

Some authors, aiming to classify several mortar types according to DTA–TG results, suggest the supplementary use of XRD and mineralogical results and they proceed to the analyses without performing any physical separation [2].

In the present work, DTA and TG–DTG have been used for analysis of historic mortars, including a wide range of ancient, Byzantine, post-Byzantine and later mortars sampled from the fortifications, monasteries and churches of Rhodes, Crete, Corfu, Mount Athos and Constantinople (Table 1). A mortar sample from Versaille Palace is used as a characteristic example of gypsum mortars. The classification of the obtained data is validated by the data of the XRD, mineralogical, chemical, mechanical and microstructural analysis performed accordingly.

2. Experimental procedure

The thermal analyses were performed with a Mettler TG 50, thermobalance, thermal analyzer system. The equipment monitors the weight loss of the mass of a 20–50 mg

Table 1
Sampling

Samples	Kind	Historical period	Location
Medieval city of Rhodes			
Rhodes 19	Joint mortar	Knights' period 15th century	St. Katherine's Guesthouse
Rhodes 13	Joint mortar	Knights' period 15th century	St. Athanasios Bastion
Rhodes 9	Crushed brick lining mortar	Knights' period 15th century	St. Athanasios Bastion
Rhodes 18	Crushed brick lining mortar	Ottoman period 16–19 cent.	St. Katherine's Guesthouse
Rhodes 8	Crushed brick lining mortar	Ottoman period 16–19 cent.	St. Katherine's Guesthouse
Rhodes 6C	Crushed brick lining mortar	Byzantine period	St. Katherine's Guesthouse
Rhodes 1C	Crushed brick lining mortar	Byzantine period	St. Katherine's Guesthouse
Rhodes 4ΘA	Hellenistic cement mortar	Hellenistic period	Old city of Rhodes
Rhodes 4ΘB	Hellenistic cement mortar	Hellenistic period	Old city of Rhodes
Rhodes 32	Surficial mortar	Knights' period 15th century	Knights' walls
Rhodes 33	Joint mortar with portlandite	Knights' period 16th century	Knights' walls
Rhodes 36	Typical lime mortar	Knights' (D'Aubusson) per.	Knights' walls
Rhodes K2	Typical lime mortar	Knights' period 15th century	Pythagora
Rhodes K3	Typical lime mortar	Knights' period 15th century	Pythagora
Venetian Fortress of Corfu			
Corfu 5	Durable joint mortar	15th century	Martinengo bastion
Corfu 8	Durable joint mortar	15th century	Savornian bastion (gate)
Corfu 17	Durable joint mortar	18th century	St. Georgios
Corfu 18	Durable joint mortar	18th century	English barracks
Corfu 28	Durable joint mortar	18th century	Cavo Sidero
Hagia sophia in Constantinople			
Hagia sophia 1.1	Crushed brick mortar	Late Byzantine (10th cent.)	North-western butresses
Hagia sophia 2.1	Durable crushed brick mortar	Byzantine (6th century)	North main arch/west point
Hagia sophia 3.1	Crushed brick mortar	Byzantine (6th century)	South-eastern abatement
Hagia sophia E3	Cement plaster	Posterior (modern)	Entrance of Hagia Sophia
Hagia sophia W1	Crushed brick mortar	Ottoman	Fortifications of the city
Byzantine and post-byzantine monasteries of Crete			
Arkadi3	Old original plaster	11th century AD	Arkadi monastery, old church, north wall

Arkadi6	Mortar	11th century AD	Arkadi monastery, explosive store house, underneath the plaster
Arkadi 8	Old original exploded mortar	11th century AD	Arkadi monastery, east wall
Preveli 4	Plaster (burned)	Restoration of 1862 AD	Monast., store-house, inner wall of the ground floor
Preveli 5	Mortar	Restoration of 1862 AD	Monast., store-house, inner wall of the ground floor
Preveli 7	Old original mortar	16th century AD	Preveli Monastery, outer wall of the store house
Chrysopigi 3	Old original mortar	15–16th century AD	Chrysopigi Monastery, houses of furnaces, inside
Chrysopigi 4	Red coloured mortar of advanced degradation	15–16 century AD	Chrysopigi Monastery, house of furnaces, inside
Agarathos 5	Old mortar	10th century AD	Agarathos Monastery, east wall of the yard
Agarathos 6	Brown coloured mortar	10th century AD	Agarathos Monastery, east wall of the yard
Agarathos 9	Soil	Contemporary	Agarathos Monastery, east, public str. to the monast.
Toplou 1	Mortar	15th century AD	Monk's cemetery, north wall
Toplou 2	Argilaceous mortar	15th century AD	Toplou Monastery, church behind the Lord's Table
Toplou 3	Fresco mortar	15th century AD	Toplou Monastery, church
Toplou 4	Crushed brick lining mortar	15th century AD	Toplou Monastery, roof of the church
Metohi vai 1	Old lining mortar	15th century AD	Terrace where grapes crushed to produce wine, internal layer
Metohi vai 2	Lining mortar	15th century AD	Terrace, internal layer
Metohi vai 3	Lining mortar	Original (1709 AD)	Terrace, external layer
Versailles	Joint mortar		
Symonos petra monastery of mount athos			
Mount athos 4	Durable cementitious mortar	14th century AD	Monastery, old southern wall
Mount athos 5	Durable cementitious mortar	14th century AD	Monastery, internal wall
Mount athos 7	Durable cementitious mortar	16th century AD	Arsenal, northern wall
Mount athos 9	Durable cementitious mortar	16th century AD	Arsenal, eastern wall

sample, when submitted to controlled heating from ambient temperature up to 1000°C (30–1000°C min^{-1}) in a static air atmosphere with a temperature gradient of 10°C min^{-1}. Simultaneously, the values of the derivative of the weight loss in relation to the time of heating are registered (DTG) where the main transformations (weight losses) occur. The value of the temperature depends on the nature of the transformation and the quantity of the substance submitted to the transformation, the heating rate and possible interferences from other substances also present.

In parallel to the thermogravimetric analysis, in the above-mentioned temperature range, differential thermal analysis (DTA) was performed with a Perkin–Elmer thermoanalyzer TG S-2 and DTA 1700. The most accurate operating condition for obtaining quantitative results is usually with a heating rate of 10°C min^{-1}. In order to save time, however, at least at the preliminary stage of the DTA analyses, a rate of 20°C min^{-1} is used, in static air atmosphere with α-alumina as reference material. The DTA curves [7], not published here, provide information about the endothermic or exothermic character of the temperature peaks. Hence the direct use of the DTG results, as quantitative analyses permitted in the present work were obtained properly at lower rates (10°C min^{-1}).

X-Ray diffraction analysis of finely pulverised samples enables the identification of the crystalline substances present when their concentration is not very low, usually under 5%. In general, the amorphous components (like the soluble silicates formed during curing of the hydraulic binding material, or the volcanic ashes of the "pozzolan"), usually very important of the hydraulic mortars, are not identifiable or could even create problems in the identification of the existing crystalline substances. That is why the XRD results alone cannot be used to determine mortars, but act as supplementary data. The analyses were performed with a Siemens D-500, X-ray diffractometer (with a graphite crystal monochromator and a Cu anticathode) based on an automatic adjustment and analysis system, with Diffract–EVA quality analysis software. Typical measurement conditions to facilitate direct comparison of various spectra, provide a diffraction interval between 2θ–5 and 2θ–60, with a step of 0.02.

3. Results and discussion

The TG–DTG and XRD analysis results from 47 samples, selected from the 200 samples analysed, are shown in the Table 2 and Fig. 1–7. Table 2 presents the % weight loss estimated from the TG–DTG curves within the temperature ranges selected to give important information. Moreover Table 2 reports the hydraulic water %, calculated in the temperature range 200–600°C, the ratio CO_2/H_2O bound to hydraulic components and the temperature of CO_2 decomposition.

3.1. Specific classification

Characteristic TG–DTG curves are presented in groups, as for the typical lime (Fig. 1), crushed brick (Fig. 2), of hot lime technology (Fig. 3), cementitious (Fig. 4), with portlandite (Fig. 1a), modern cement (Fig. 4a) and gypsum mortars (Fig. 5).

3.1.1. Typical lime mortars (Fig. 1)

The TG demonstrates the absence of any important weight loss before the calcite decomposition ranging between 820–840°C and releasing over 30% CO_2 (equivalent to over 68% $CaCO_3$). The mortars do not present any hygroscopic behaviour, since they contain adsorbed water more or less around 1% during heating up to 120°C (mean temperature of weight loss ~ 60°C). The XRD results show mortars consisting mainly of calcite (~ 80%) and quartz. The binding material is finely crystallized calcite, totally carbonated. The aggregates are mainly calcitic consisting of microfossils, fossil fragments and coarse clastic quartz grains [8]. A large group of Rhodes mortars are typical lime sand mortars of binding-to-inert ratio 1/2. In that case, two main peaks are observed, the one portlandite (460°C) and that of calcite transferred to 765–780°C. The extremely high levels of water bound to hydraulic components > 14%, is characteristic. In the cases of mortars with (crystalline) portlandite present, where carbonation is inhibited (Fig. 1a), structures of a higher density and strength result (Rhodes 33) [8].

3.1.2. Crushed brick–lime mortars (Fig. 2)

Among the great variety of traditional mortars, crushed brick mortars are of specific interest due to their elevated bearing capacity. The resemblance of the several homologous mortars coming from buildings from the Byzantine, Venetian and Ottoman periods in Rhodes [9], Crete [10] and Hagia Sophia [11] could be a useful tool for revealing traditional production technology. The so called "pozzolanic" character of crushed brick mortar is attributed to the adhesion reactions of physico-chemical character occurring at the ceramic–matrix interface [9, 12]; their nature depends both on the type of ceramic and the calcium hydrate content of the mortar. The observed reactions could probably be attributed to calcium silicate formations at the interface along the brick fragment, acting as the silicate source and membrane and the lime, which makes the interfacial surface alkaline and causes the chemical reaction [6, 9]. The penetration of lime into the ceramic and the consequent reaction transforms the microstructure of the ceramic by transforming the pore radii into smaller pores, decreasing the total porosity and augmenting the apparent density. The reduction of the pore radii confirms the cementitious character of the mortar matrix [10], imparting high strength to the mortar [13].

From the XRD results, it is evident that the binding material of the samples is exclusively calcitic, showing slight differences as far as different aggregate fragments (quartz and plagioclase of various types) are concerned. The presence of calcium silicate hydrate (CSH), calcium aluminate hydrate (CAH), calcium aluminum chloride hydrate (CACH), tobermorite (Tb), illite (Il) and montmorillonite in significant content in the matrix confirms the cementitious character of the latter. These results indicate either interface reactions, or the origin of the lime from argillaceous limestones.

Microscopic observations give ample evidence of products of boundary reactions. Reaction rims at the ceramic–matrix interface are dispersed in the form of veins along the matrix, as if they fill the vacancies and discontinuities of its structure. Fine to medium grained aggregates, mainly quartz and plagioclase, varying in % by surface, are embedded in the calcitic matrix [9].

Table 2
TG–DTG (weight loss per temperature) and XRD (crystalline phases) results

Mortar Samples	Weight loss per temperature range/%					Hydraulic water/%	CO_2/ hydraulic water	T_{CO_2}/°C	XRD results[a]
	< 120	120–200	200–400	400–600	> 600				
Crushed brick and lime mortars									
Rhodes 9	1.52	0.50	1.72	2.02	33.86	3.74	9.05	820	Cc, Q, Pg, Tb, CSH
Rhodes 18	1.04	1.04	2.17	2.68	29.92	4.85	6.17	820	Cc, Q, Pg , CSH, Msc
Rhodes 8	1.87	0.62	1.66	2.74	25.91	4.40	5.89	815	Cc, Q, Pg, CSH, Msc
Rhodes 6C	2.53	0.99	2.18	3.02	30.35	5.20	5.84	805	Cc, Q, Do, Pg, Msc, Tc, CACH, Tb
Rhodes 1C	1.65	0.94	2.23	2.68	27.79	4.91	5.66	805	Cc, Q, Pg, CSH, CAH, CACH, Mnt, Tb
H. Sophia 1.1	1.98	0.68	1.98	2.80	19.47	4.78	4.07	780	Cc, Q, Pg, CAH, Mnt, Msc
H. Sophia 2.1	1.19	0.45	1.50	3.25	11.22	4.75	2.36	760	Cc, Q, Pg, CSH, Mnt
H. Sophia 3.1	1.14	0.48	1.39	2.13	11.02	3.52	3.13	760	Cc, Q, Pg, CSH, Mnt
H. Sophia W1	2.28	1.38	1.99	3.19	14.00	5.18	2.70	760	Cc, Q, Pg, CAH
Toplou 4	1.55	0.70	1.31	2.24	6.26	3.55	1.76	780	Cc, Q, Pg, CSH
Metochi 2	1.41	1.00	2.93	3.38	22.63	6.31	3.59	780	Cc, Q, Pg
Cementitious mortars									
Rhodes 4ΘA	4.46	2.58	3.92	11.67	12.35	15.59	0.79	740	Cc, Q, Do, Pg, Gy, Chl, CSH
Rhodes 4ΘB	4.14	2.09	3.79	11.25	12.87	15.04	0.86	740	Cc, Q, Do, Pg, Gy, Chl, CSH
Rhodes 32	3.27	3.04	3.97	6.54	19.63	10.51	1.87	775	Cc, Q, Pg, Gy, Tb
Rhodes 36	0.97	1.76	2.20	4.22	24.34	6.42	3.79	800	Cc, Q, Do, Gy, Pg
Corfu 5	3.53	1.01	1.70	2.75	7.39	10.14	0.73	800	Cc, Q, Pg, Do, K
Corfu 8	1.43	0.61	1.36	4.07	19.02	5.43	3.50	740	–
Corfu 17	0.89	0.16	2.96	3.55	18.16	6.51	2.80	820	Cc, Q, CASH
Corfu 18	1.12	0.31	7.16	5.51	10.74	12.67	0.85	750	Q, Cc, Pg, CSH
Corfu 28	0.80	0.37	2.84	3.80	13.12	6.64	1.98	780	Cc, Q, CASH, Il
Arkadi 6	2.56	1.42	3.13	5.70	14.95	8.83	1.69	750	Cc, Q, Msc, Chl, Pg, CAH
Arkadi 8	1.24	1.39	2.08	2.35	11.76	4.43	2.65	790	Cc, Q, Msc, Pg, Chl, Prt, CAH
Preveli 5	0.98	0.77	1.89	3.23	13.24	5.12	2.59	765	Q, Cc, Msc, Pg, Prt, Chl
Preveli 4	1.37	0.98	2.70	2.70	30.44	5.40	5.64	800	–
Chrysopigi 3	0.90	0.49	1.31	1.75	16.65	3.06	5.44	780	–
Agarathos 6	1.11	0.36	1.44	2.33	22.87	3.77	6.07	800	Cc, Q, Msc, Chl, Pg, Tb
Toplou 2	1.73	0.48	1.73	3.65	17.63	5.38	3.28	770	–

Typical lime mortars									
Rhodes 19	1.25	0.54	1.36	1.57	37.14	2.93	12.68	835	Cc, Q
Rhodes 13	0.69	0.11	0.96	1.06	39.33	2.02	19.47	840	Cc, Q
Rhodes K2	0.56	0.47	1.22	1.60	33.28	2.82	11.80	830	Cc, Q, Do
Rhodes K3	0.81	0.47	1.33	1.66	33.25	2.99	11.12	825	Cc, Q, Do
Metochi 3	0.94	0.47	1.30	1.60	32.17	2.90	11.09	840	Q, Cc, Pg, Msc, Chl
Arkadi 3	1.41	0.65	1.74	1.39	36.31	3.13	11.60	840	Cc, Q, Msc, Chl, Prt, Pg
Preveli 7	1.48	0.49	1.58	1.47	32.61	3.05	10.69	800	–
Agarathos 5	0.59	0.39	1.41	1.61	33.46	3.02	11.08	800	–
Toplou 1	0.66	0.44	1.49	1.37	38.00	2.86	13.29	825	–
Toplou 3	0.23	0.30	0.60	0.00	42.23	0.60	70.38	820	–
Mortars with portlandite									
Rhodes 33	1.17	1.55	2.01	10.05	18.01	12.06	1.49	765	Prt, Cc, Q, K
Metochi 1	1.89	1.71	3.15	10.90	17.11	14.05	1.22	780	Q, Cc, Msc, Pg,Gy, Prt
Gypsum mortars									
Versailles	1.77	5.23	0.97	0.88	3.78	1.85	2.04	730	–
Hot lime technology									
M. Athos 4	1.06	0.76	1.52	2.13	18.24	3.65	5.00	790	Cc, Q, Pg, Do
M. Athos 5	0.55	0.21	1.17	1.54	20.34	2.77	7.34	785	Cc, Q, Pg, Do, Tc
M. Athos 7	0.76	0.21	1.56	1.26	29.02	2.82	10.29	815	Cc, Q, Pg, Chl, Do, Tc
M. Athos 9	0.99	0.99	3.56	2.76	30.14	6.32	4.77	805	Cc, Q, Pg, Chl, Do, Msc
Modern cement mortar									
H. sofia E3	1.75	0.91	2.02	3.49	9.34	5.51	1.69	760	–
Raw materials									
Agarathos 9	1.12	1.81	1.30	2.50	27.30	3.80	7.18	800	–
Chrysopigi 4	2.16	0.88	2.68	4.00	3.82	6.68	0.57	700	Cc, Q, Pg, Msc, Gy

[a] Cc: calcite, Q: quartz, Do: dolomite, Pg: plagioclase (albite), Gy: gypsum, Prt: portlandite, Chl: chlorite, CAH: calcium aluminate hydrate, CSH: calcium silicate hydrate, CACH: calcium aluminum chloride hydrate, CASH: calcium aluminum silicate hydrate, Tb: tobermorite, Mnt: montmorillonite, Tc: talc, Il: illite, K: kaolinite, Msc: muscovite.

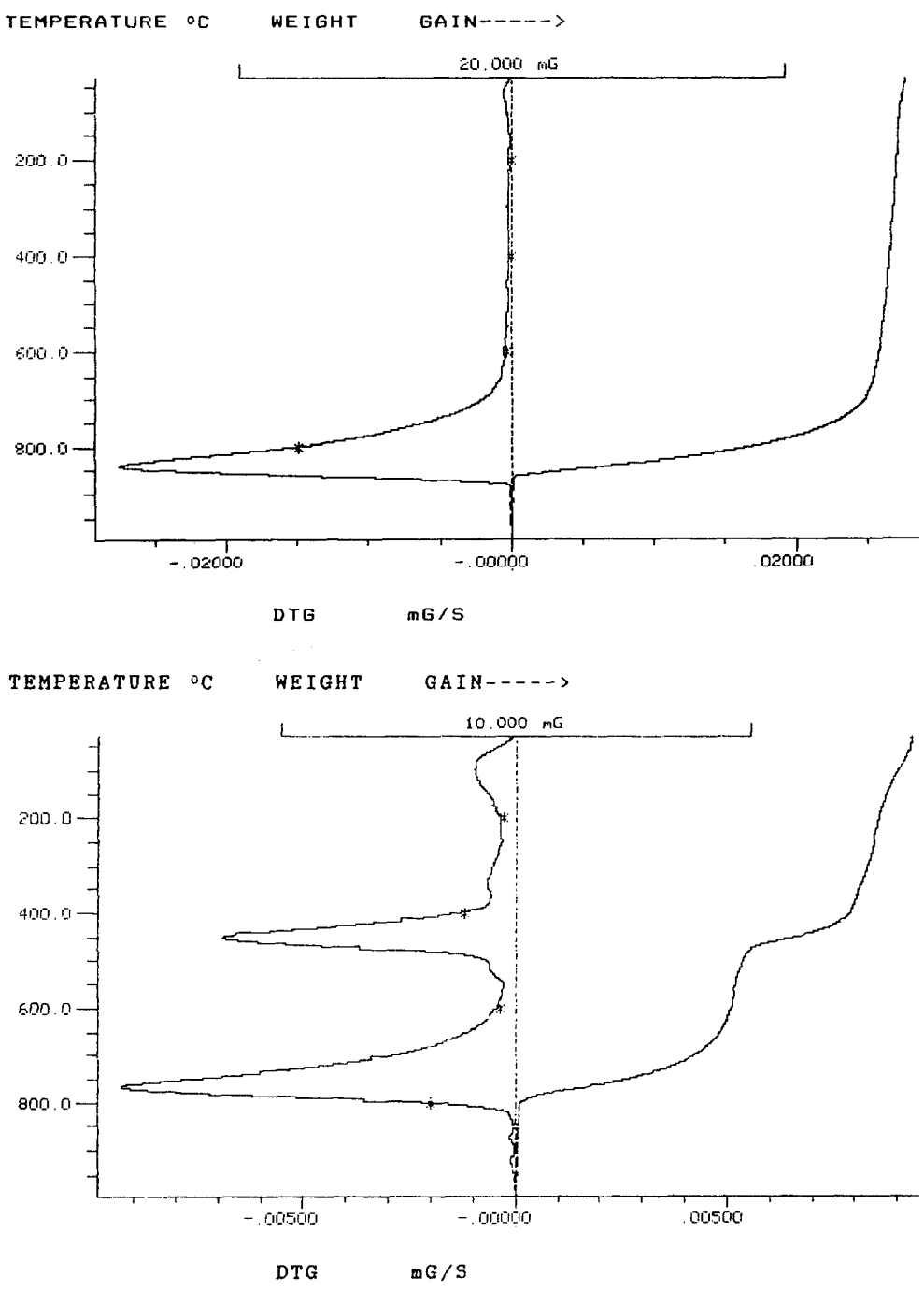

Fig. 1. Typical lime mortar and mortar with portlandite (a).

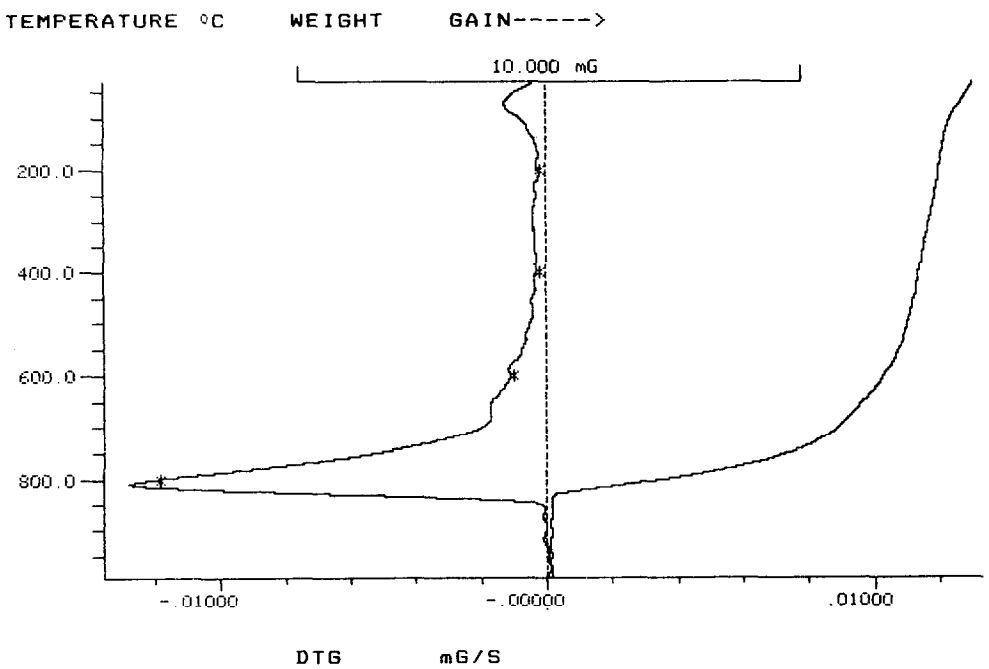

Fig. 2. Crushed brick and lime mortar.

The DTG demonstrates a series of peaks indicating: weight loss (~ 1–2%) of adsorbed water at about 80°C; weight loss (over 3.5%) of water bound to the several calcium aluminum silicate hydrates (CSH, CAH, Tb, CACH) of about 200–260°C, 480–520–580°C, the later when argillaceous compounds like montmorillonite or illite are traced; and weight loss (ranging from 6–33%) of CO_2 during the calcite decomposition occuring between 760–820°C.

Crushed brick-lime mortars of several technologies span binding-to-inert material ratios between 1/4, 1/3 and 1/2.5.

3.1.3. Hot lime technology mortars (Fig. 3)

From our previous results, Mount Athos mortars could be classified above the usual tensile strength levels presented by hydraulic lime mortars, attaining even higher values than those presented by crushed brick-lime mortars [14]. According to the X-ray diffraction results, the mortars consist mainly of calcite with embedded quartz clastic grains, feldspars and phyllosilicate minerals. Typically the same magnesium–argillosilicate minerals are found in the binder as well.

Clear evidence of a cementitious matrix is given by scanning electron micrographs showing the typical hydraulic components. The cementitious character of the Mount Athos mortars could be attributed to hot lime technology. Finely ground magnesium

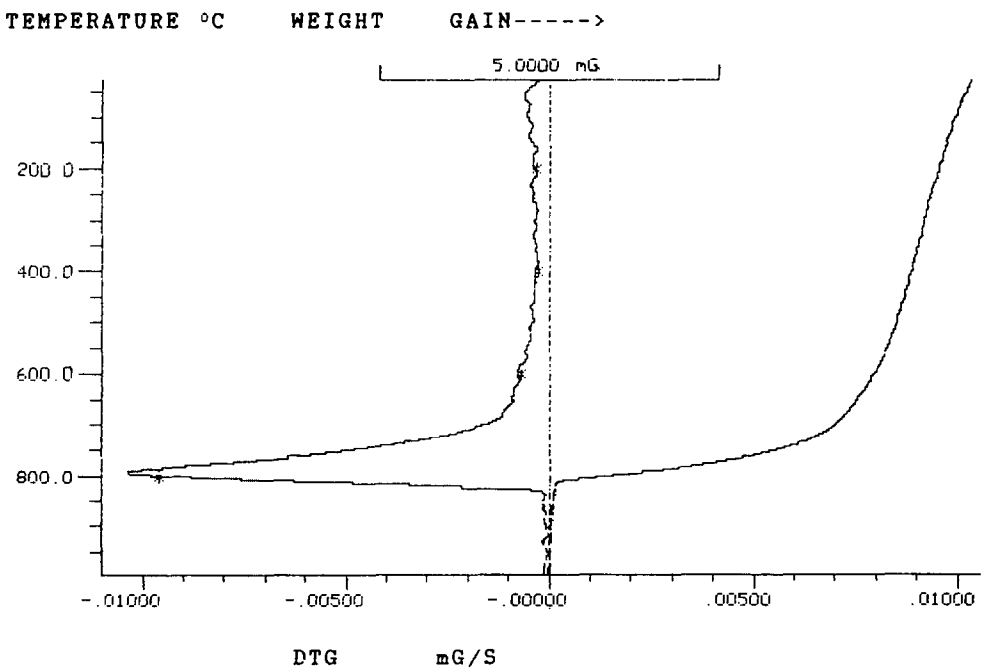

Fig. 3. Hot lime technology.

aluminosilicate dust of the montmorillonitic clays in the area, could have been mixed and reacted with the in situ slaked lime in the process of the so called "pozzolanic" reactions.

The results of thermogravimetric analysis show, after < 1% absorbed water between 50 and 120°C, a 3–6% weight loss in the temperature range between 200 and 600°C, for all the samples, attributed to water bound to aluminum silicate hydrate or CSH minerals (peaks 200–600°C). In the case of the sample 9, intense endothermic effects (DTA) [14] around 400°C, indicate the dehydroxylation of clays, most probably reacting to hydrated products with the "in situ" slaked lime. Carbonates show distinctive endothermic peaks between 785 and 815°C, most probably due to the decomposition of the cementitious matrix of "pozzolanic" character rich in magnesium.

A mixture of 1/2.5–1/3 lime aggregates has been estimated with 1/5 active clay admixtrues/inert aggregates.

3.1.4. Cementitious mortars (Fig. 4)

"Opus Caementicium" or the so-called cementitious mortars are described by Vitruvius [15] as an artificial conglomerate of gravel with sand and lime cement. The view that the basic silicates are formed by burning and then hydrolyzed by water yielding lime and hydrated silicates, was propounded by A. Winkler and has since been

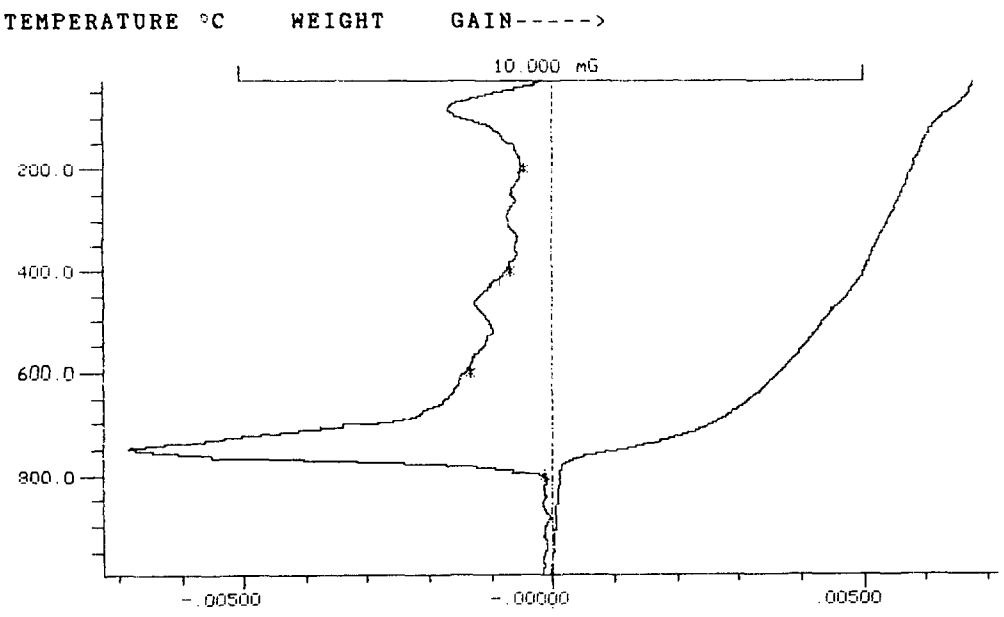

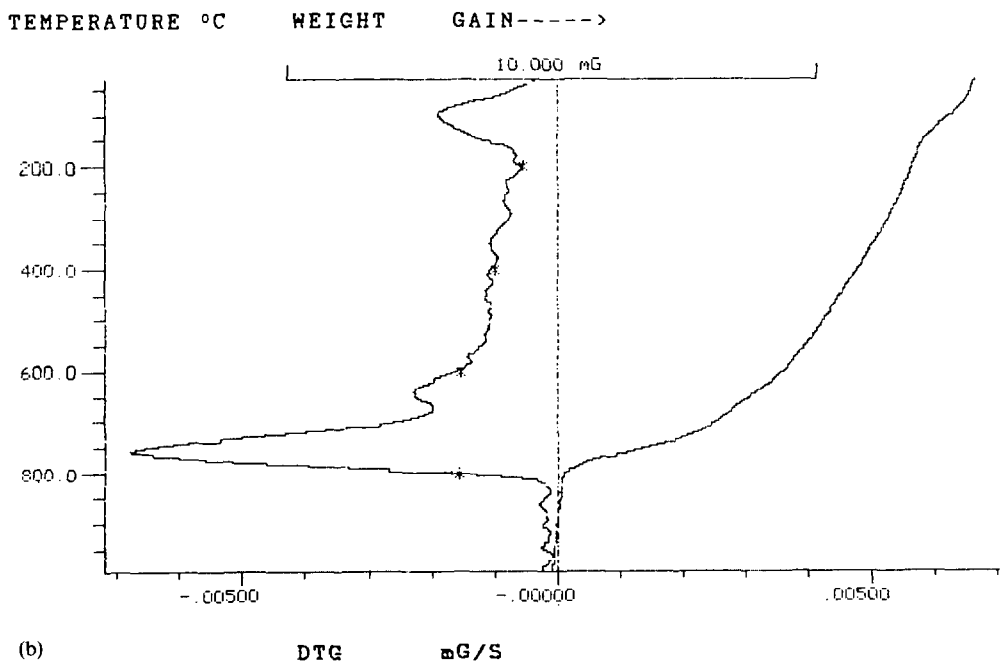

Fig. 4. Cementitious mortar. Modern cement mortar (a) and raw material (b).

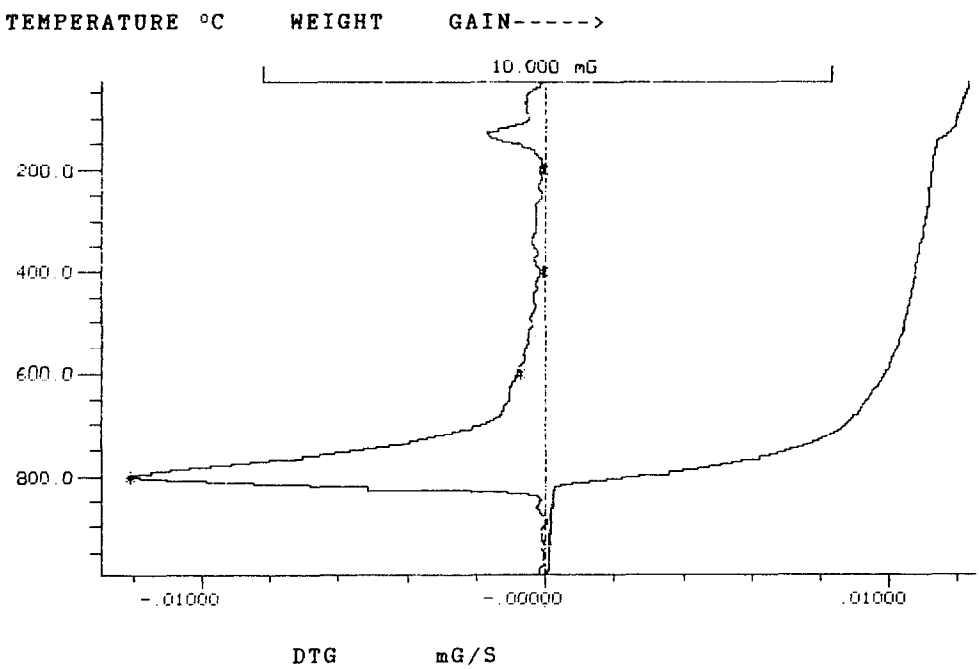

Fig. 4. (continued).

fully established [16]. Raw clays consist essentially of a group of hydrated aluminum silicates, though alumina may be replaced to varying extents by ferric oxide, and to a lesser extent by bases such as MgO, Na_2O and CaO (TG of raw material, Fig. 4b). In the case under study, a wide range of mortars from Rhodes (Hellenistic cement) [7], from Corfu (Venetian and English period) [178] and from Byzantine and post-Byzantine monasteries of Crete [17], present these features.

XRD results show the presence of CSH, CASH, CACH, chlorite (Chl), Tb, Prt and Il. The TG curves show a weight loss due to: adsorbed water (1–4%) at about 80°C; water bound (3–16%) to aluminum silicate hydrates, presenting peaks at 280, 450 and 480°C—especially when CSH is detected—and at 550 and 580°C—when CASH or CACH is detected. These are characteristic peaks of the so called "pozzonalic" reactions. $CaCO_3$ decomposition occurs at about 740–820°C. The weight loss of CO_2 varies mainly between 10 and 20% indicating lime aggregate ratios at around 1:3.

In distinction, the modern cement plaster from Hagia Sophia (Fig. 4a) shows the characteristic peaks of transformation concerning gypsum and adsorbed water (< 120°C), CASH (520–600°C) and $CaCO_3$ at 760°C.

3.1.5. Mortars with gypsum (Fig. 5)

For the sake of classification the Versailles Palace mortar sample was analysed to show the characteristic peak of gypsum dehydration at 130–160°C, followed by the peak of $CaCO_3$ decomposition at 730°C.

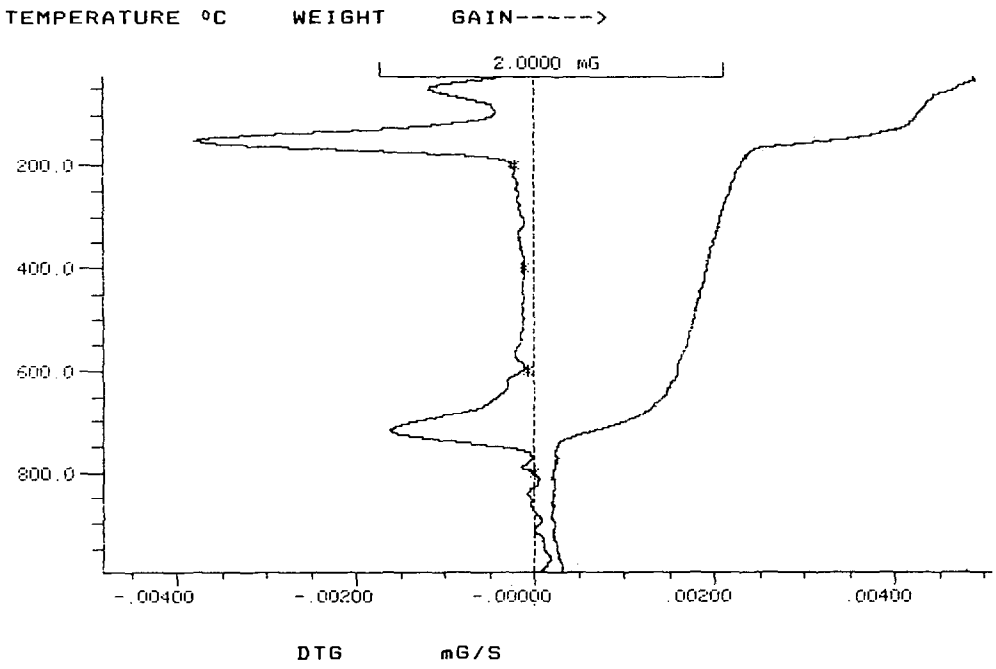

Fig. 5. Gypsum mortar.

3.2. General trends

Fig. 6 presents the ratio of CO_2/H_2O (hydraulic water) which inversely expresses the hydraulic character of the mortar in relation to the CO_2 (weight loss %). The inverse trend of hydraulicity of the mortar samples is shown to augment exponentially with CO_2. The cementitious mortars are concentrated at the bottom, the crushed brick and hot lime mortars in the middle of the curve and the typical lime mortars at the upper right in ratios of $> 10\%$ and $CO_2 > 32\%$.

Fig. 7 presents weight loss % the water bound to hydraulic components in relation to CO_2 %, two areas of mortars are discerned:

1) The typical lime mortars above the 1:2 lime/aggregate ratio, showing however, less than 3% water bound to "hydaulic" components (weight loss between 200 and 600°C).
2) The so called "pozzolanic" mortars, including all the categories of crushed brick, cementitious, hot lime, portlandite mortars or modern cement.

In the "pozzolanic" area two subgroups could be distinguished: one with over 10% hydraulic water content, where the more condensed and higher strength mortars are identified, and the other subgroup with less than 5% hydraulic water content.

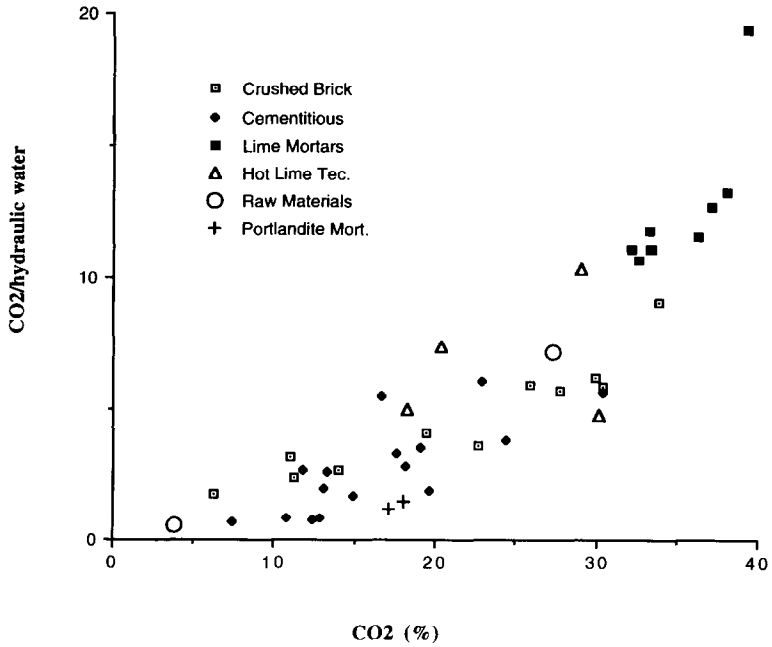

Fig. 6. The inverse ratio of hydraulicity in relation to CO_2.

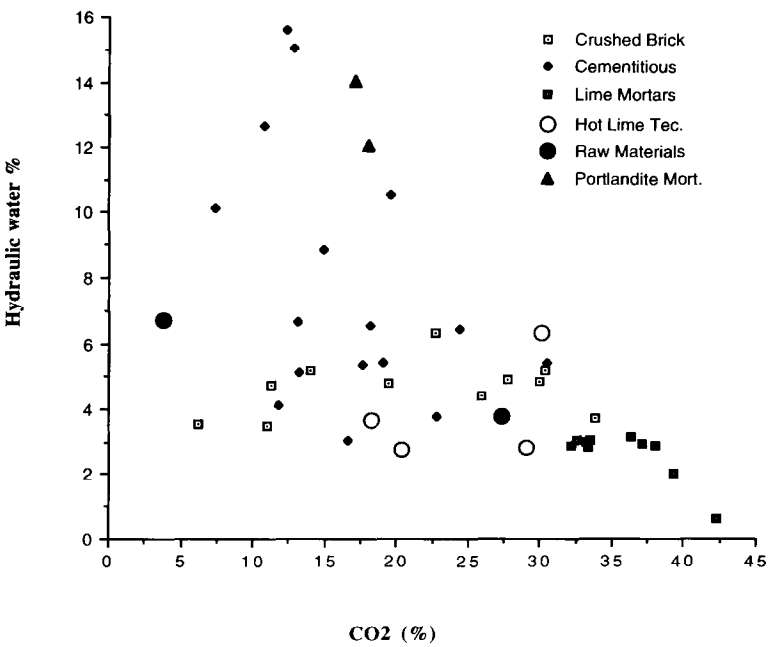

. Fig. 7. Water bound to hydraulic components in relation to CO_2.

4. Conclusions

Generally the water bound to hydraulic components in combination with the CO_2 (in weight loss %) discerns two groups of mortars: the typical lime and the hydraulic type. The specific classification of mortars in groups of characteristic transformations, indicated by weight loss against temperature, enables discrimination between typical lime, cementitious, with crushed brick, with portlandite, with gypsum, with modern cement or of hot lime technology, mortars.

Mineralogical, microstructural, mechanical and technological data could provide further evaluation criteria.

References

[1] R.C. Mackenzie, in Differential Thermal Analysis 2, 1st edn., Academic Press, London, 1970.
[2] G. Chiari, M.L. Santarelli and G. Toracca, Materiali e Strutture, 3 (1992) 111–137.
[3] T. Wiedmann, Tonind. Ztg., 82 (1958) 331–337.
[4] D.A. Holdridge, Trans. Br. Ceram. Soc., 64 (1965) 211–231.
[5] J.E. Adams and W.A. Kneller, in Marinos and Koukis (Eds.) Engineering Geology of Ancient Works, Monuments and Historical Sites, Balkema, Rotterdam, 1988, pp. 1019–1026.
[6] A. Bakolas, R. Bertoncello, G. Biscontin, A. Moropoulou, E. Zendri and E. Tondello, in Materials Issues in Art and Archaeology IV (Mater. Res. Soc. Proc., 1994, in press).
[7] A. Moropoulou, A. Bakolas and K. Bisbikou, Science and Technology for Cultural Heritage, 1994, in press.
[8] A. Moropoulou, G. Biscontin, P. Theoulakis, E. Zendri, A. Bakolas, K. Bisbikou, A. Theodoraki and N. Chondros, in M.J. Thiel (Eds.) Conservation of Stone and other Materials, (Proc. Int. Cong. UNESCO/RILEM, Paris, 1993) pp. 394–401.
[9] A. Moropoulou, G. Biscontin, K. Bisbikou, A. Bakolas, P. Theoulakis, A. Theodoraki and T. Tsiourva, in Calcestruzzi antichi e moderni: storia, cultura e tecnologia, Proc. Scienza e Beni Culturali IX, Bressanone, 1993, pp. 415–429.
[10] A. Moropoulou, A. Theodoraki, K. Bisbikou and M. Michailidis, in Materials Issues in Art and Archaeology IV, Mater. Res. Soc. Proc., 1994, in press.
[11] A. Moropoulou, Hagia Sophia Crushed Ceramic Mortars, Bogasizi University Lecture, 17 March, 1994.
[12] R.A. Livingston, P.E. Stutzman, R. Mark and M. Erdik, in P.B. Vandiver, J.R. Druzik, G.S. Wheeler and I.C. Ftreestone (Eds.) Materials Issues in Art and Archaeology III, Mater. Res. Soc. Proc. 267, Pittsburgh, PA, 1992, pp. 721–736.
[13] A.S. Cakmak, A. Morpoulou, J. Soil Dyn. Earthquake Eng., 1994, in press.
[14] A. Moropoulou, Th. Tsiourva, K. Bisbikou, A. Bakolas, J. Constr. Build. Mater., 1994, in press.
[15] Vitruvius, in The Ten Books on Architecture (M.H. Morgan Trans., Dover Publications, New York, 1964) p. 45.
[16] A. Winkler, Prakt. Chem., 67 (1856) 444.
[17] A. Moropoulou, K. Bisbikou, A. Theodoraki, P. Michailidis, J. Photos, Th. Poulgouras and P. Bibas, in Natural and Cultural Heritage, Proc. Int. Conf. UNESCO, Crete, 1993.
[18] A. Moropoulou, P. Theoulakis and S. Kefalonitou, Study of the Weathering and the Proper Conservation–Protection Intervention Concerning the Venetian Fortress of Corfu, Technical report, 1992.